Journal of Template

Vol. 00, No. 0, 0000

Effect of Local Periodic Disturbance on Mixing Layer at Exit of Two-Dimensional Jet*

Masashi ICHIMIYA** Toshihiro KATO*** and Tsutomu MORIMOTO****

**Institute of Technology and Science, The University of Tokushima,
2-1 Minami-Josanjima-cho, Tokushima-shi, Tokushima, 770-8506 Japan
E-mail: ichmiya@me.tokushima-u.ac.jp
***The Chugoku Electric Power Co.,Inc.
****Institute of Technology and Science, The University of Tokushima

Abstract

The laminar-turbulent transition of a mixing layer induced by oscillating flat plates at an exit of a two-dimensional nozzle was experimentally investigated. A mixing layer was formed between the jet from the nozzle and the surrounding quiescent fluid. The plates oscillated vertically in relation to the mean flow. The oscillation frequency was two orders of magnitude smaller than the fundamental frequency of the velocity fluctuation. Mean and fluctuating velocity components in the streamwise and normal directions were measured by hot-wire anemometers. The oscillation was found to be effective in enhancing the mixing, though the amplitude was the same order as the momentum thickness of the boundary layer at the nozzle exit. The disturbance traveled downstream as the convective instability, though it was damped only far downstream. The downstream development rate of fluctuating velocity in the normal component was larger than that in the streamwise one. Thus, the need for linear instability analysis of non-parallel flow was suggested. Streamwise variations were examined in the fluctuating velocity and perturbation energy production and convection rates, which contribute to the velocity. The streamwise variation in the streamwise component did not correspond to that of the normal component.

Key words: Mixing Layer, Transition, Turbulence, Jet, Oscillating Plate, Periodic Disturbance, Absolute/Convective Instability, Velocity Distribution

1. Introduction

Laminar-turbulent transition phenomenon has been investigated for many years since it occurs many times in the natural world and industrial machines. Recently, an example of the transition in a wake of turbine cascades was shown(1). The wake is an example of the free shear flow without constraint by a solid wall. The transition in such free shear flow is an important issue in the industrial world.

Many kinds of free shear flow have been shown other than the wake flow(2)(3). One example is a mixing layer formed between the jet just behind a nozzle and the surrounding quiescent fluid. This type of mixing layer is classified as ‘jet boundary’ in Ref. (4). The present study concerns the laminar-turbulent transition in the mixing layer as one of the fundamental problems in the transition in free shear flow.

This type of flow which enters and flows out of a domain is called ‘open flow’(5). In the stability analysis of the open flow, disturbance is assumed as a modal type such as $A(y)\exp[i(kx-\omega t)]$. Then, the disturbance is discriminated as temporal or spatial developments. After the disturbance has been amplified, it is analyzed as a nonlinear

*Received XX Xxx, 200X (No. XX-XXXX)
[DOI: 00.0000/ABCDE.2006.000000]

disturbance. Recently, a new analysis has been developed in which the disturbance is discriminated as absolute or convective instability[5]~[9]. Moreover, this disturbance is discriminated as a local or global instability. In the analysis, attention is focused on the non-normality in equations.

Regarding the transition just after the nozzle, many studies on many types with and without disturbances have been introduced[10]. An acoustic wave is an example of a high-frequency disturbance[11]~[23]. Since the velocity of sound is much faster than the flow velocity in these experiments, the acoustic disturbance propagates throughout the whole flow field instantaneously. The resulting instability can be said to be absolute instability. On the other hand, another type, the convective instability, is induced by a disturbance produced by vibrating objects in a local position and was convected downstream[24]~[27]. Recently, a study which used a piezo film actuator and promoted mixing of the mixing layer was published[28]. Its amplitude (0.5～2 mm) was relatively large. In these studies, however, detailed streamwise variations of velocity distributions have not been demonstrated.

In many studies, the excitation frequency was set equal to the fundamental frequency of the velocity fluctuation in the early stage of the unforced transition. The ideal flow field involving the present transition is the free shear flow with a parallel free stream[29]. In the linear stability theory with this parallel free stream, this type of flow is the most unstable among all kinds of free stream, and then becomes unstable due to the disturbance with extremely low wave number, i.e., long wavelength in contrast with the boundary layer[30]. In the present disturbance, the disturbance vorticity is created by a plate oscillation and may be convected with the free stream. Therefore, the order of the wavelength of the disturbance can be estimated as U_m / f_e with the free stream velocity, U_m, and the oscillation frequency, f_e. The long wavelength corresponds to the low frequency. The low frequency, 5 Hz, adopted in the present study is two orders of magnitude lower than the common fundamental frequency of several hundred Hz, which is observed in the early stage of many experiments[10][13][18][19]. Moreover, it is also smaller than the frequency of the coherent structure in the mixing layer of a few hundred or thousand Hz[31][32]. The distribution of fluctuating vorticity in such a long wavelength, i.e., the process during large eddy changes into a smaller eddy which exists in turbulent flow, has not been investigated thoroughly. Therefore, studies which can cover a wide range of wavelength corresponding to that of the fluctuating vorticity are awaited. The problems with low frequency disturbance are expected to be solved also in the industrial world, for example, in an air oscillation whose frequency is less than audio frequency. The low-frequency disturbance has been shown to persist far downstream[33], though the only examples are in the turbulent jets[34]~[36].

The present study deals with a local disturbance which is made by fence-like plat plates which oscillate and protrude vertically in relation to the main jet. The protrusion is so small that the velocity fluctuation due to the net protrusion is almost the same as without it. The downstream variation of the distribution of mean and fluctuating velocity components is investigated in detail in the region where fluctuation developed spatially until self-preservation is established. The mixing layer has local convective instability and its spatial development depends on the type of forced disturbance, so it acts as a noise amplifier[5]. We focus on two points: how far the forced periodic oscillating disturbance persists and how the flow field is changed by the convective instability. Additionally, the downstream variations in production, convection and dissipation rates of the perturbation energy are obtained, for they have not been reported previously.

Nomenclature

b : half-width
f_e : oscillation frequency of oscillating plates = 5 Hz
h : nozzle exit height = 10 mm

U, u : mean and fluctuating velocity component in streamwise direction
U_0 : velocity at x = 5 mm, y = 0
U_m : local velocity on centerline, y = 0
V, v : mean and fluctuating velocity component in normal direction
u', v' : root mean square value of u, v
x, y : coordinate system
δ_ω : vorticity thickness
ε : perturbation energy dissipation rate
$\bar{*}$: time average of quantity $*$

2. Experimental Apparatus and Methods

A blowing-type wind tunnel was used in which air is blown into the measurement section from a two-dimensional nozzle exit of aspect ratio 31 (310 mm in width and 10 mm in height, h). The flow at the exit has a velocity gradient within a region of 1.6 mm from the upper and lower nozzle walls, respectively, while the velocity is kept constant in the other region, 7 mm. The velocity profile measured by a hot-wire anemometer almost coincided with the Blasius profile. Two side walls 310 mm apart for a whole measurement section were installed to secure the two-dimensionality of the flow. Moreover, a ceiling wall was installed whose height from the nozzle centerline is equal to the vertical distance between the centerline and the laboratory floor. Mean velocity profiles are measured at some spanwise positions downstream of the nozzle, and they well coincided with each other.

Two oscillation plates 2 mm in thickness were equipped across the whole width to make a disturbance in the upper and lower mixing layer. An rpm-controlled motor was used for the plate oscillation. The revolution was transmitted to cams by belts, and then the revolution of the cams was transmitted to the protrusion of each oscillating plate. A photo sensor signal corresponding to the angle of rotation of this cam was output, and the phase of the plate oscillation was detected with it. Figure 1 shows the left and right cams and the photo sensor on the right side viewed from downstream. The plates oscillate perpendicularly and sinusoidally in relation to the flow at a frequency, f_e, of 5 Hz. This frequency is two orders of magnitude smaller than the fundamental frequency in the natural transition process, which is, approximately, 400 Hz. If the oscillation frequency is one order of magnitude smaller, any differences might not have appeared. On the other hand, if it is more than three orders of magnitude smaller, the frequency is less than 0.5 Hz and the flow field may be the same as stationary flow.

The upper half of the flow field and coordinate system are shown in Fig. 2. The bottom

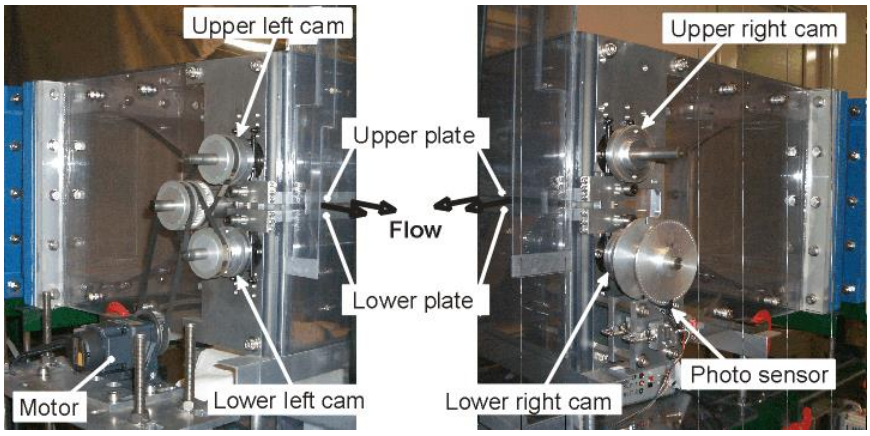

(a) (b)

Fig. 1 Nozzle and cam mechanism viewed from left (a) and right side (b)

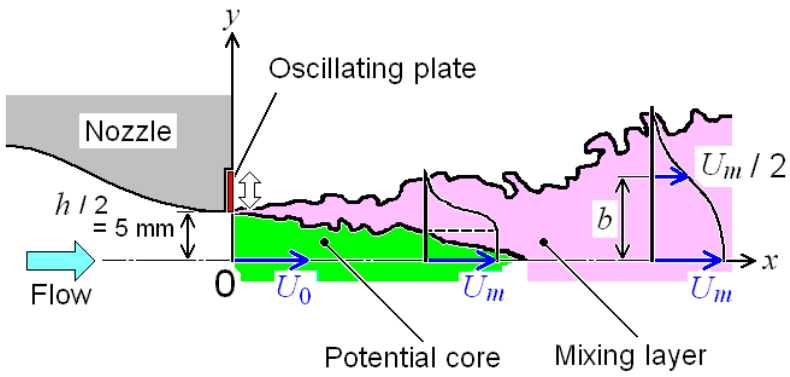

Fig. 2 Schematic diagram of two-dimensional mixing layer and coordinate system

of the oscillating plate in Fig. 2 becomes flush with the nozzle wall surface when it rises to its highest point, and then descends from the surface by 0.25 mm at most. In other words, the nozzle height 10 mm is decreased 0.5 mm at the moment when the two plates simultaneously protrude maximally from the nozzle respective surfaces. The bottom of the oscillating plate in Fig. 2 displaces within the region $0.95 \leqq y/(h/2) \leqq 1.00$. The value 0.25 mm is smaller than the displacement thickness in the exit boundary layer, 0.46 mm and is of the same order as the momentum thickness, 0.18 mm. The value was chosen so that no additional disturbance occurred when the plates protrude and are at rest. Actually, the distribution of the fluctuating velocity at the nozzle exit when both plates protrude and are at rest was almost the same as when both plates do not protrude and are rather smaller than when both plates oscillate. Therefore, an additional disturbance due to a mere protrusion of the plates can be ignored, that is, the oscillation of the plates may induce the disturbance. In fact, when the protrusion doubled to 0.50 mm each, the fluctuating velocity increased more than when without protrusion, although the flow rate through the nozzle area was always constant irrespective of the protrusion. The velocity on the nozzle centerline, U_0, increases/decreases correspondingly with the decrease/increase of the nozzle sectional area. On the other hand, the velocity near the nozzle edge shows phase reversal with U_0, which always makes the flow rate through the nozzle constant. Next, to check the effect of noise of the motor and cam when the plates oscillate, the spectral of the noise was analysed. The wind tunnel noise and plate oscillation noise did not interact, that is, the plate oscillation noise may not affect the growth of the periodic velocity fluctuation.

Two types of experiments were performed. In one, the plates remained stationary so that the plates do not narrow the nozzle exit section (stationary state). In another, the plates oscillated at a frequency of 5 Hz (oscillating state). In any case, the Reynolds number was 5000 based on the nozzle exit velocity without oscillation, $U_0 \simeq 7.5$ m/s, and nozzle exit height, h. The Strouhal number based on plate oscillation frequency, f_e, and nozzle exit velocity, U_0, was about 2×10^{-4}. All measurements were done at the spanwise position, $z = 20$ mm, where the streamwise velocity profile was most symmetric with respect to the nozzle centerline. X-shaped hot-wire probes with two tungsten sensing elements, each 5 μm in diameter and 1 mm in length, were used for the measurements. Output voltage was sampled at a sampling frequency of 5 kHz for about 52 seconds. This interval is equivalent to about 260 oscillations when the plates oscillate. The measurements were conducted in a range of $y \geqq 0$. Results are shown here in the range $x/h \leqq 10$, where the mean velocity profiles did not become similar, and $x/h = 20$ where the profiles had become completely similar.

3. Results and Discussion

3.1 Variations of Mean Quantities with Oscillation Disturbance

First, the effects of the plate oscillation on the mean quantities are described. Notations in the velocity distributions below are listed in Table 1.

Figure 3 shows mean velocity profiles in the streamwise component. The potential core region where the velocity normalized by the nozzle exit velocity, U_0, equals unity persists until $x/h \simeq 6$ or 3 in the stationary and oscillating states, respectively. Therefore, the potential core disappears earlier with plate oscillation. Moreover, velocity in the region

Table 1 Symbols in Fig. 3 – 6, 8 – 10, and 12 – 16

symbol	x / h	symbol	x / h	symbol	x / h
△	0.5	▽	4	◇	10
◭	1	▽	5	◆	20
▲	1.5	▼	6		
○	2	□	7		
◑	2.5	◨	8		
●	3	■	9		

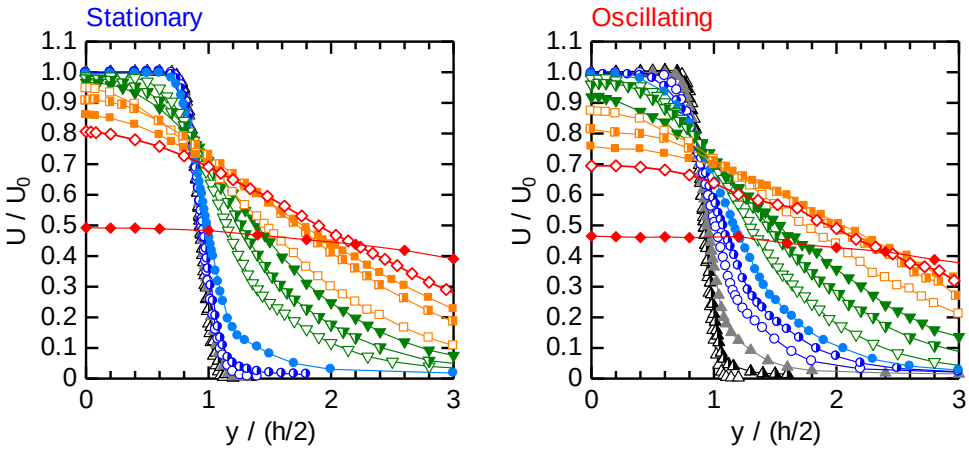

Fig. 3 Mean velocity profiles in streamwise component

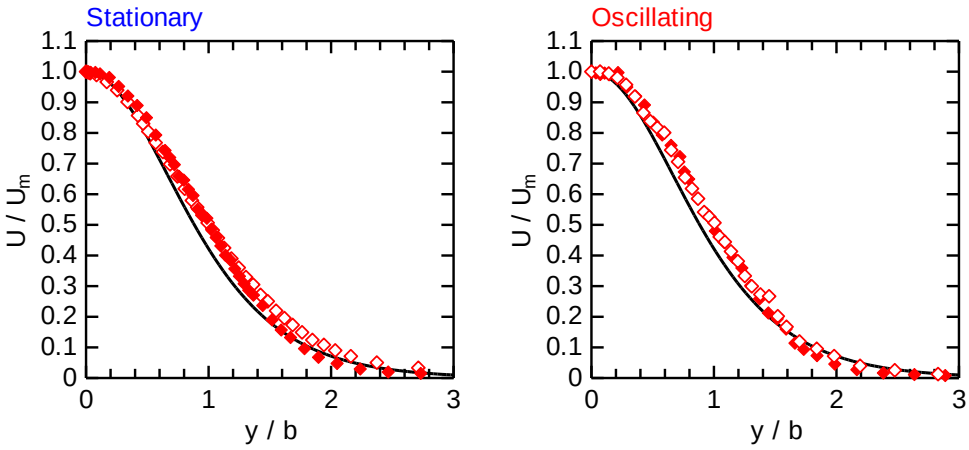

Fig. 4 Mean velocity profiles in streamwise component with similar coordinates

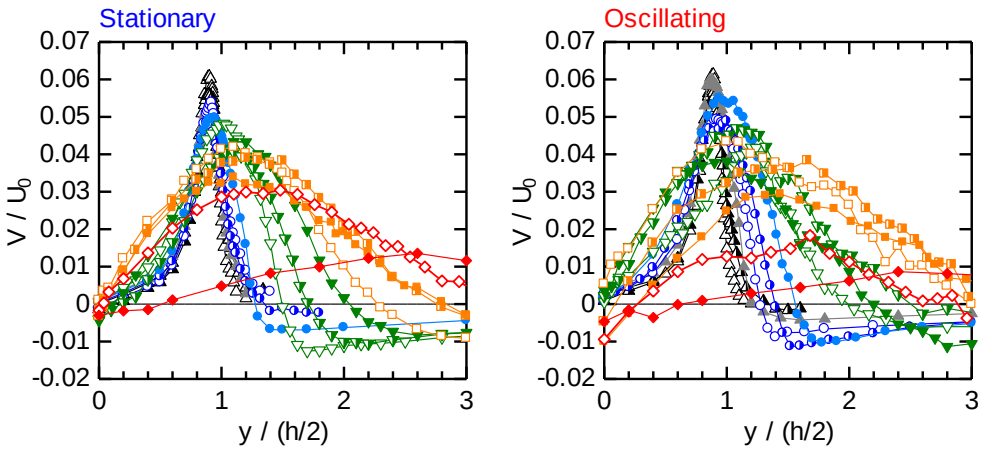

Fig. 5 Mean velocity profiles in normal component

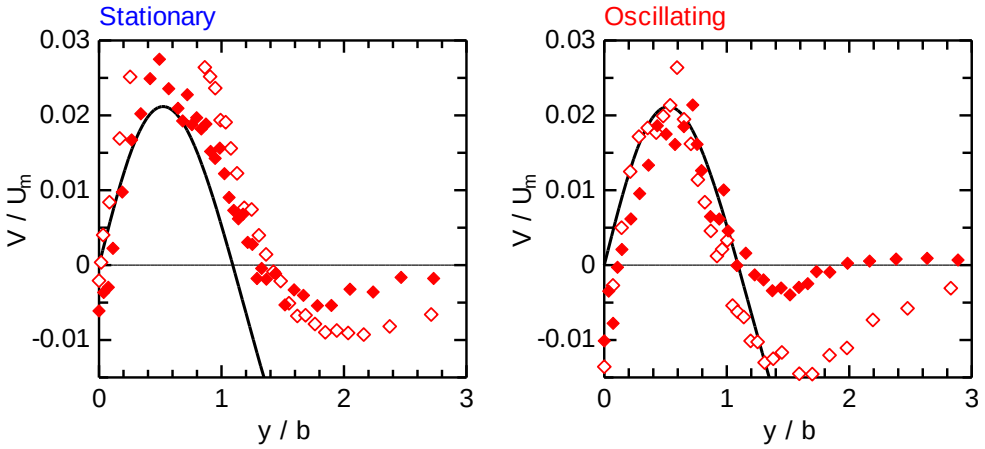

Fig. 6 Mean velocity profiles in normal component with similar coordinates

away from the nozzle edge, $y/(h/2) > 1$, increases more in the oscillation state. Thus, plate oscillation with a small amplitude such as 0.25 mm can promote mixing of the jet. In the region 4 < x/h, however, both profiles correspond with each other because of such a small amplitude.

Figure 4 shows theoretical profiles[37] when the jet is self-preserved and compares with the experimental profiles. The profile is calculated with an empirical formula later in Fig. 7, $b = 0.138(x - x_0)$ (x_0 is a virtual origin). Far downstream and after the disappearance of the potential core, $x/h = 10$, the experimental one coincides with the theoretical one.

Figure 5 shows mean velocity profiles in the normal component. At first, the velocity distributes in a narrow region in the vicinity of the nozzle edge. Then the value gradually increases near the center of the nozzle and the maximum value decreases with the disappearance of the potential core. In the outer region the values become negative, indicating that the surrounding fluid is entrained toward the mixing layer.

Figure 6 compares the theoretical profiles of the mean velocity in the normal component[37]. In the region where the theoretical profile takes a positive value, $0 < y/b < 1$, the experimental values coincides with the theoretical one at $x/h = 20$ and 10 in the stationary and oscillating states, respectively. Away from the nozzle the theoretical value takes a largely negative value, though the experimental one finally tends to zero. The discrepancy may be attributed to the fact that the interface of the jet has not been considered in the theory and that the jet has been assumed to extend infinitely. There may have not

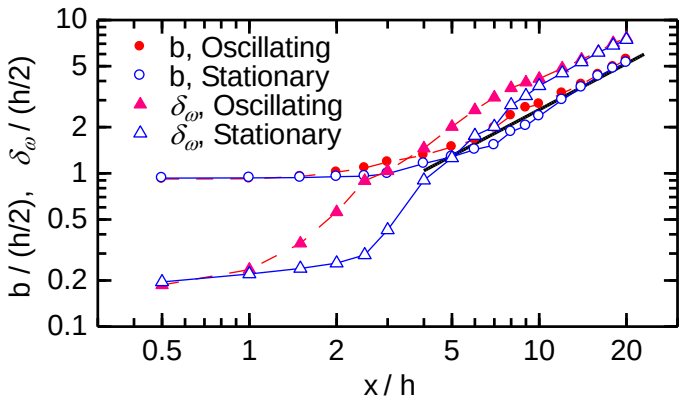

Fig. 7 Half-width and vorticity thickness

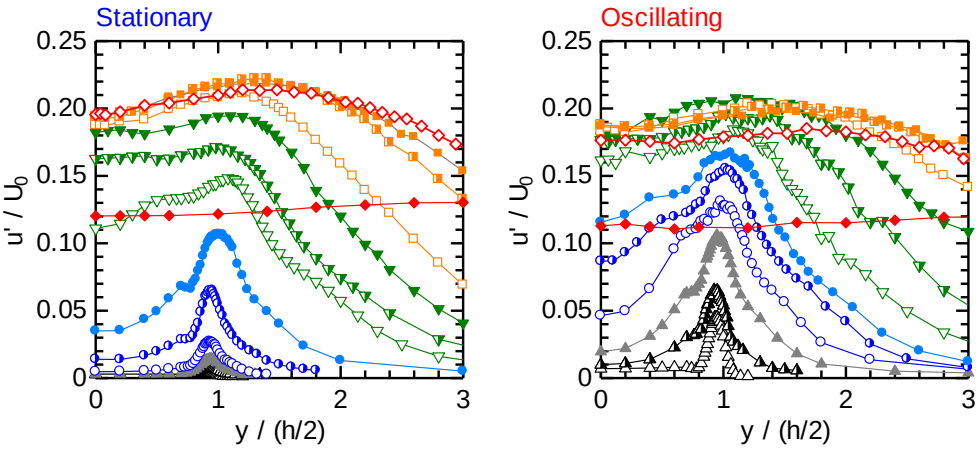

Fig. 8 Distributions of fluctuating velocity component in streamwise direction

been a definite policy for the treatment of the interface[38].

Figure 7 shows distributions of a half-width and vorticity thickness. First, due to the existence of the potential core, mean velocity gradient, $\partial U/\partial y$, exists within a narrow region near the nozzle edge, the half-width exists there. Then, the half-width gradually increases in accordance with the reduction of the potential core and expansion of the mixing layer region. The increase is faster in the oscillating state than the stationary state, though the difference disappears finally.

The vorticity thickness is estimated by $-U_m / (\partial U/\partial y)_{max}$, where $(\partial U/\partial y)_{max}$ is the maximum value in the mean velocity gradient at a local x/h. The thickness is small at first, and then increases in accordance with the reduction of the potential core and expansion of mixing layer region. In the oscillating state, the increase is faster than the stationary state due to the fast reduction of the potential core, though the difference disappears finally. Such an effect may affect the vortex formation and breakdown within the mixing layer. According to the velocity signals and power spectrum of the fluctuating velocity[39], the subharmonic fluctuation appears earlier in the oscillating state, i.e., the oscillation promotes the amalgamation of the vortices. From the downstream variation of the half-width and vorticity thickness, the oscillation disturbance may amplify with the convective instability at first, then become stable so it attenuates and effect of the disturbance disappears. That is, the behavior of the present flow field as the noise amplifier does not always persist because of the small amplitude such as 0.25 mm without additional disturbance due to the plate protrusion.

3.2 Variations of Fluctuating Quantities with Oscillation Disturbance

During the laminar-turbulent transition process in the mixing layer, the linear region appears at first where disturbances grow exponentially and a periodic fluctuation, i.e., a fundamental wave, is observed[40]. Next, the nonlinear region appears where the harmonic and subharmonic waves of the fundamental wave are observed. At last, the irregular region appears where an irregular fluctuation dominates. In the present section, the growth of the fluctuation and effect of the oscillation on it are considered in the respective regions.

Figure 8 shows distributions of rms value of the fluctuating velocity component in the streamwise direction. Just after the nozzle the fluctuating velocities are rather high only in the vicinity of the nozzle edge in the stationary state, and then the values rapidly increase downstream. This increase occurs more upstream in the oscillating state. The detailed increase is considered in Fig. 11. The fluctuating velocity also increases in the vicinity of the nozzle centerline in accordance with the potential core reduction. This increase continues until it overshoots and finally slightly decreases to reach a constant value. The final values in the stationary and oscillating states are almost the same.

Figure 9 shows distributions in rms values of the fluctuating velocity component in the normal direction. It also increases downstream, and the increase occurs earlier in the oscillating state than in the stationary state, especially in the region of $2 \leqq x/h \leqq 3$. This increase of the fluctuating velocity in the normal direction is larger than that of the streamwise direction. The increase in the perturbation energy production and convection

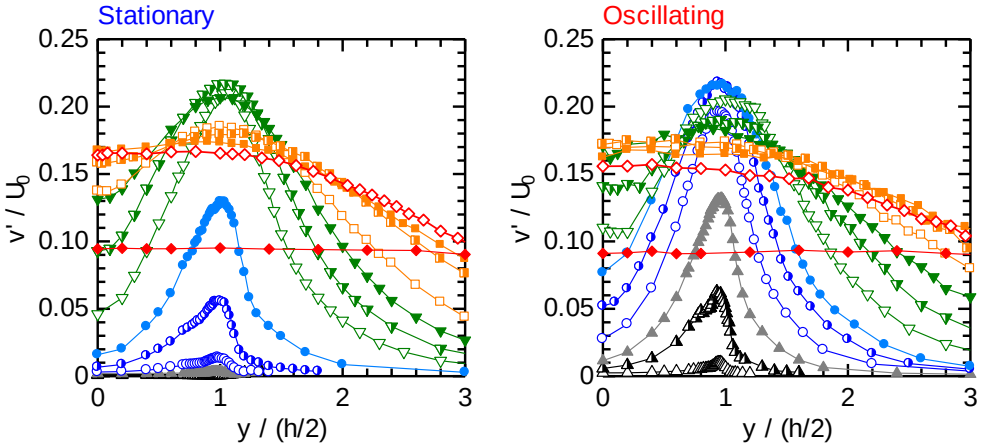

Fig. 9 Distributions of fluctuating velocity component in normal direction

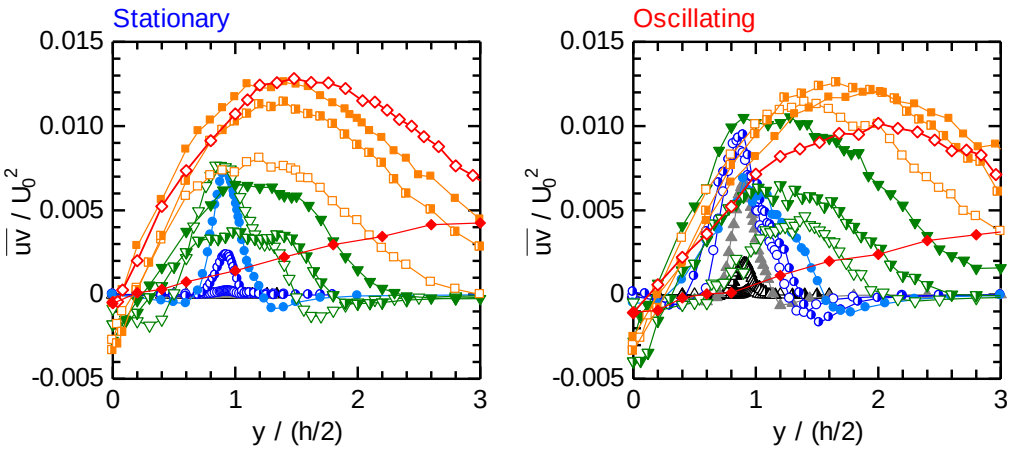

Fig. 11 Distributions of Reynolds shear stress component

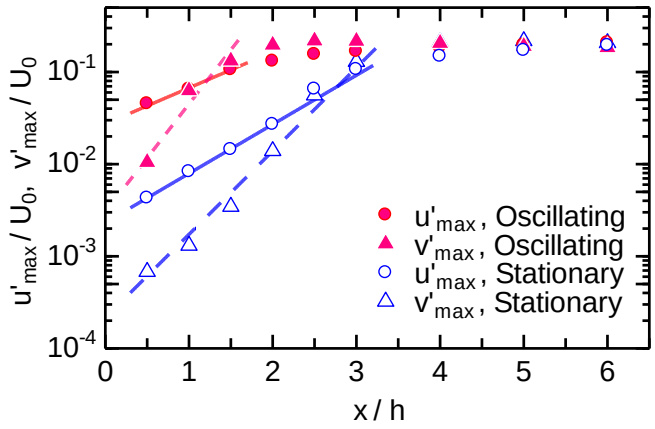

Fig. 11 Streamwise variation of maximum fluctuating velocities

rates within this region, later shown in Fig. 14 and 15, are larger than those in the streamwise direction later shown in Fig. 12 and 13. The increase may contribute to the fluctuating velocity. The plate oscillation in the normal direction may cause the increase in the normal direction. Just after the nozzle, the value of this component is larger than the streamwise component, though its final value is smaller than that.

Figure 10 shows distributions of Reynolds shear stress. In the oscillating state, the value once overshoots, and then slightly decreases downstream.

To investigate such downstream growth of the fluctuation, maximum values in the normal distribution of u' and v' at respective station x/h are obtained in Fig. 8 and 9, respectively. Figure 11 shows the downstream variation of the maximum values. In the stationary state, distributions in both streamwise and normal components are on linear in the $x/h \leqq 3$ region, that is, the fluctuating velocity grows exponentially. Therefore, this is the linear region of the present flow. The growth rate in the normal component is larger than in the streamwise one. After the linear region the growth rate decreases. In the oscillating state, the exponential region exists in the region of $x/h \leqq 1.5$; the growth rate of the respective component is almost the same as that of the same component in the stationary state. In the region of $4 \leqq x/h$, the maximum values are almost the same in both states because of the small amplitude.

Freymuth obtained the streamwise growth rate of the streamwise fluctuating velocity u' by the slope of the straight line in a semi-log plot like Fig. 11[(11)]. He assumed the stream function ψ of the small disturbance in the linear equations in the parallel flow to be an exponential function. As he did in the streamwise component, u', the growth rate of the normal component, v' was obtained and turned out to be the same form. The experimental fact that the slope of the straight line in v'_{max} is steeper than that in u'_{max} contradicts the above theoretical result. This implies that the parallel flow assumption is not valid in the present flow. Therefore, an important issue is to estimate how parallel the present flow is. Chomaz showed that the parallel flow assumption is valid when the streamwise gradient of a characteristic local length scale such as a displacement thickness, a momentum thickness, a vorticity thickness, etc., is much smaller than unity[(9)]. Also, in accordance with Chomaz, when the vorticity thickness in Fig. 7 is adopted as the length scale, the $d\delta_\omega/dx$ increases monotonically in the linear region above and finally reaches above 0.1 both in the stationary and oscillating states. This shows that the parallel flow assumption is not valid in the present flow. The function of the small disturbance in a linear stability theory in non parallel flow has not been established. The discrepancy between the present experiment and the usual theory may be attributed to the non parallelism of the flow. Although variations of the maximum values at respective station x/h are shown in Fig. 11, the value in the fixed normal

position e.g., $y/(h/2) = 1$ showed the same results, that is, the growth rates are different between the streamwise and normal components and the same both in the stationary and oscillating states with the same component.

The nonlinear region starts from the end of the linear region. The end of the nonlinear region, i.e., the beginning of the irregular region, may be regarded as the station where the instantaneous velocity signal has become irregular, and may be estimated as $x/h = 15$ and 10 in the stationary and oscillating state, respectively.

Near the end of the linear region the fluctuating velocity reaches a fairly large value as seen in Fig. 11. Therefore, the perturbation energy production and convection rates due to the second-power term of the perturbation may be critical even in the linear region. The boundary-layer-approximated perturbation energy budget equations are[41]:

$$U\frac{\partial}{\partial x}\frac{\overline{u^2}}{2}+V\frac{\partial}{\partial y}\frac{\overline{u^2}}{2}=-\overline{u^2}\frac{\partial U}{\partial x}-\overline{uv}\frac{\partial U}{\partial y}+\frac{1}{\rho}\overline{p\frac{\partial u}{\partial x}}-\frac{\partial}{\partial y}\frac{\overline{u^2v}}{2}+\nu\overline{u\nabla^2 u} \quad (1)$$

$$U\frac{\partial}{\partial x}\frac{\overline{v^2}}{2}+V\frac{\partial}{\partial y}\frac{\overline{v^2}}{2}=-\overline{uv}\frac{\partial V}{\partial x}-\overline{v^2}\frac{\partial V}{\partial y}+\frac{1}{\rho}\overline{p\frac{\partial v}{\partial y}}-\frac{\partial}{\partial y}\frac{\overline{v^3}}{2}-\frac{\partial}{\partial y}\frac{\overline{vp}}{\rho}+\nu\overline{v\nabla^2 v} \quad (2)$$

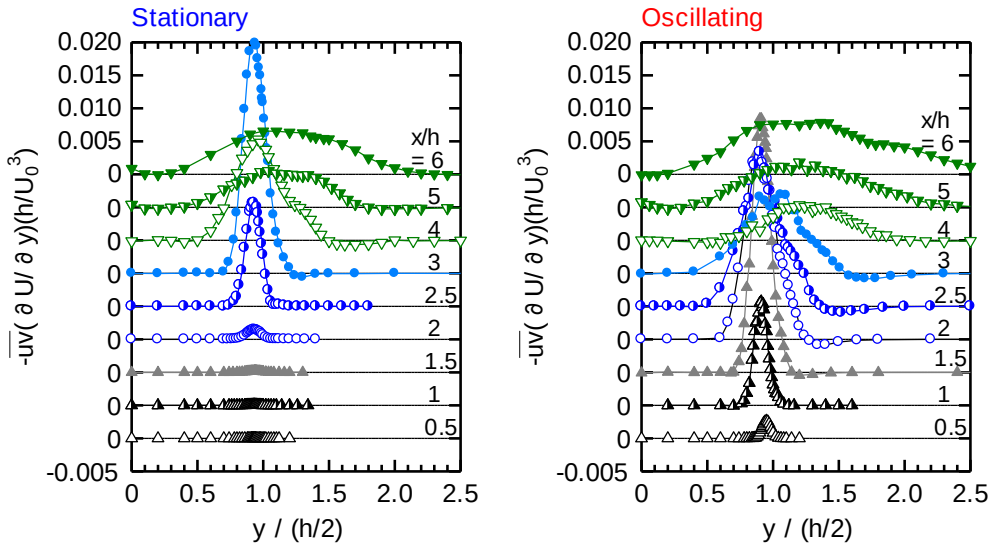

Fig. 12 Perturbation energy production rates in streamwise component

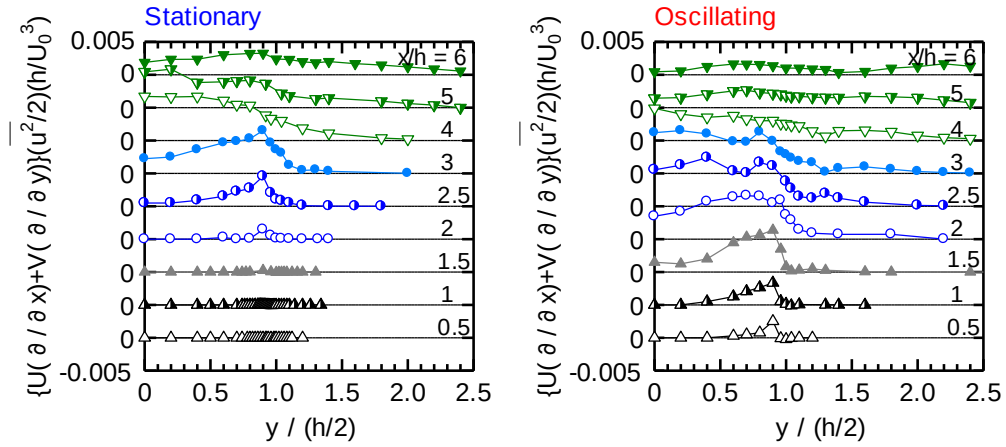

Fig. 13 Perturbation energy convection rates in streamwise component

Where in Eq. (2), the production rate based on the streamwise gradient of the normal mean velocity, $\partial V/\partial x$, which had been ignored in Ref. (41), are also shown. These equations are the same whether u and v are regular or irregular.

At first, for the streamwise component, $\overline{u^2}/2$, the production rate based on the normal gradient, $-\overline{uv}\partial U/\partial y$, and the sum of the two convection rates, are shown in Fig. 12 and 13, respectively. They are seen in the region within the nonlinear region, $x/h \leqq 6$. The streamwise and normal gradients are estimated by the experimental data. All rates are normalized by the nozzle exit velocity, U_0, and nozzle exit height, h. Among all production rates, quantities based on the streamwise gradient were negligible compared with that based on the normal gradient. In addition, among all convection rates, the $V\partial/\partial y$ term was one order of magnitude smaller than the $U\partial/\partial x$ term. Moreover, the $W\partial/\partial z$ term might be sufficiently smaller than the others. The production rates in Fig. 12 increase until x/h = 3 and 1.5 in the stationary and oscillating states, respectively. These stations are the end of the region where the fluctuating velocity increases exponentially in the respective state. After the region the distributions suddenly change, and in the nonlinear region the rates change gradually.

The convection rates in Fig. 13 increase even in the nonlinear region until x/h = 4 and 2.5 in the stationary and oscillating states, respectively. The fluctuating velocity itself, u', continued to increase until x/h = 8 and 6 in the stationary and oscillating states, respectively, though not shown in the figure. Therefore, a factor other than the perturbation energy

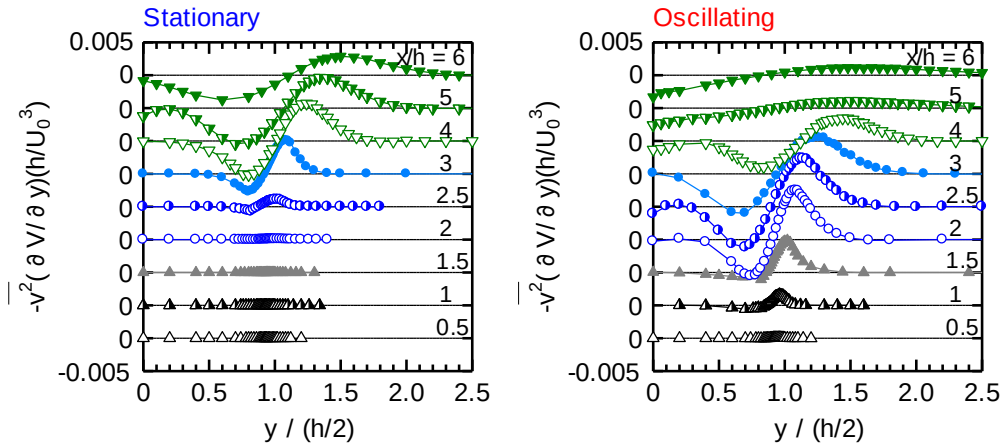

Fig. 14 Perturbation energy production rates in normal component

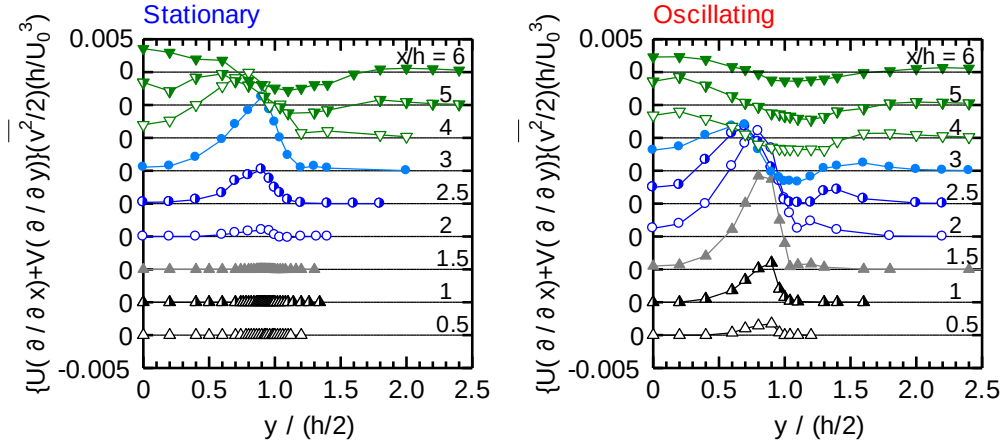

Fig. 15 Perturbation energy convection rates in normal component

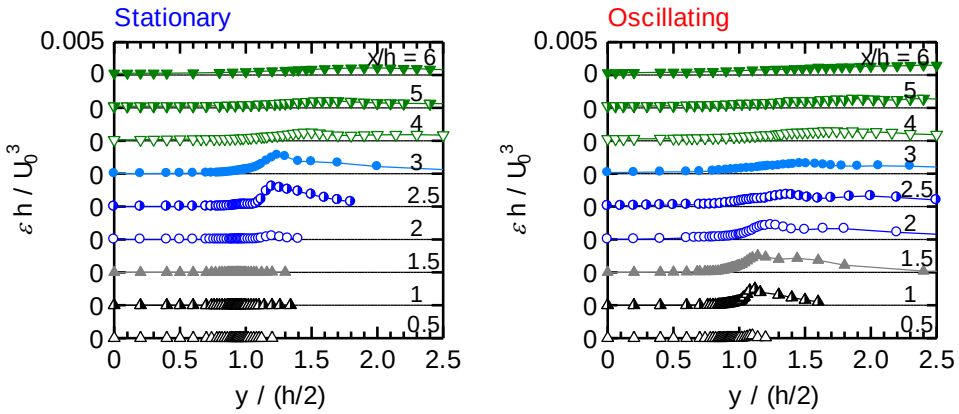

Fig. 16 Perturbation energy dissipation rates

production and convection rates might contribute to the increase of *u*' in the nonlinear region such as the energy redistribution rate between components due to the three-dimensionalization of the perturbation.

Next, the production and convection rates in the normal energy $\overline{v^2}/2$ are shown in Fig. 14 and 15, respectively. The production rates in Fig. 14 become maximum at *x*/*h* = 4 and 2.5 in the stationary and oscillating states, respectively. These stations are both in the nonlinear region.

The convection rates in Fig. 15 become maximum at *x*/*h* = 3, which is the end of the linear region, and 2 within the nonlinear region in the stationary and oscillating states, respectively. The fluctuating velocity itself, *v*', becomes maximum at almost the same stations, i.e., *x*/*h* = 5 and 2.5 in the stationary and oscillating states, respectively. Therefore, the production and convection rates may well contribute to the increase of *v*'. These types of increase in *u*' and *v*' may not have been mentioned before in the literature.

Figure 16 shows the perturbation energy dissipation rate, which is an important factor as the production and convection rates. As usual, the dissipation rate was estimated from $15\nu\overline{(\partial u/\partial t)^2}/U^2$, by assuming an isotropy and frozen turbulence. As different from the production and convection rates in Figs. 12-15, the dissipation rate is for the total component, $(\overline{u^2}+\overline{v^2}+\overline{w^2})/2$. The rate becomes maximum at *x*/*h* = 2.5 and 1.5, in the stationary and oscillating states, respectively. Hence, the stations with maximum dissipation virtually coincide with those of the production of $\overline{u^2}/2$ in both states. In both states, the condensed distribution suddenly changes and the maximum decreases near the end of the linear region. The Kolmogorov scale eddy scale $\eta_K = (\nu^3/\varepsilon)^{1/4}$, increases around there. This means that the spatial variation developed in the linear region may become gradual.

The results for the fluctuating quantities above show that the present small local disturbance greatly affects the fluctuating quantities.

4. Conclusions

A small amplitude disturbance without additional fluctuation from the protrusion itself was locally created with low frequency, and then this disturbance was forced to enter a mixing layer formed at the exit of a two-dimensional nozzle. The laminar-turbulent transition in the mixing layer is investigated experimentally. The following conclusions within this Reynolds number are obtained.

(1) Mixing and expansion of the mixing layer can be promoted by a disturbance. The small amplitude such as the momentum thickness at the exit of the nozzle is effective for expansion of the mixing layer.

(2) The present disturbance amplifies as the convective instability at first, and then

attenuates convectively downstream; finally, the difference between the stationary and oscillating states disappears.
(3) In the linear region the growth rate in the velocity fluctuation is larger in the streamwise component than in the normal one. To explain this, the need for linear stable analysis based on the non parallel flow is implied.
(4) The perturbation energy production, convection and dissipation rates which contribute to the streamwise component become maximum near the end of the linear region and decrease downstream, though fluctuating velocity itself continues to increase downstream. Factors other than the production, convection and dissipation rates may contribute to the increase in velocity fluctuation. On the other hand, production, convection and dissipation rates which contribute to the normal component become maximum in the nonlinear region, and the fluctuating velocity itself becomes maximum around there.

Acknowledgments

The assistance of Messrs J. Tamatani, T. Osaki, J. Sugihara, T. Shinkai, K. Takeuchi, A. Okajima and S. Kamada of the University of Tokushima is gratefully acknowledged. The authors also appreciate the kind instruction and constant encouragement of Prof. I. Nakamura of Nagoya University.

References

(1) Durbin, P. and Wu,. X., Transition Beneath Vortical Disturbances, *Annual Review of Fluid Mechanics*, Vol. 39 (2007), pp. 107-128.
(2) Rajaratnam, N., *Turbulent Jets* (1976), Elsevier.
(3) Shakouchi, T., *Jet Flow Engineering -Fundamentals and Application-* (2004), Morikita Shuppan(in Japanese).
(4) Schlichting, H. and Gersten, K., *Boundary-Layer Theory, 8th Revised and Enlarged ed.* (2000), p. 652, Springer.
(5) Huerre, P. and Monkewitz, P. A., Local and Global Instabilities in Spatially Developing Flows, *Annual Review of Fluid Mechanics*, Vol. 22 (1990), pp. 473-537.
(6) Huerre, P. and Monkewitz, P. A., Absolute and Convective Instabilities in Free Shear Layers, *Journal of Fluid Mechanics*, Vol. 159 (1985), pp. 151-168.
(7) Couairon, A. and Chomaz, J. M., Absolute and Convective Instabilities, Front Velocities and Global Modes in Nonlinear Systems, *Physica D*, Vol. 108, No. 3 (1997), pp. 236-276.
(8) Chomaz, J. M., Transition to Turbulence in Open Flows: What Linear and Fully Nonlinear Local and Global Theories Tell Us, *European Journal of Mechanics B/Fluids*, Vol. 23, No. 2 (2004), pp. 385-399.
(9) Chomaz, J. M., Global Instabilities in Spatially Developing Flows: Non-Normality and Nonlinearity, *Annual Review of Fluid Mechanics*, Vol. 37 (2005), pp. 357-392.
(10) Sato, H., Experimental Investigation on the Transition of Laminar Separated Layer, *Journal of the Physical Society of Japan*, Vol. 11, No. 6 (1956), pp. 702-709.
(11) Freymuth, P., On Transition in a Separated Laminar Boundary Layer, *Journal of Fluid Mechanics*, Vol. 25, Pt. 4 (1966), pp. 683-704.
(12) Sato, H., Further Investigation on the Transition of Two-Dimensional Separated Layer at Subsonic Speeds, *Journal of the Physical Society of Japan*, Vol. 14, No. 12 (1959), pp. 1797-1810.
(13) Sato, H., The Stability and Transition of a Two-Dimension-al Jet, *Journal of Fluid Mechanics*, Vol. 7 (1960), pp. 53-80.
(14) Browand, F. K., An Experimental Investigation of the Instability of an Incompressible, Separated Layer, *Journal of Fluid Mechanics*, Vol. 26, Pt. 2 (1966), pp. 281-307.

(15) Miksad, R. W., Experiments on the Nonlinear Stages of Free-Shear-Layer Transition, *Journal of Fluid Mechanics*, Vol. 56, Pt. 4 (1972), pp. 695-719.
(16) Makita, H., Ohtani, H. and Ishizumi, K., Acoustic Control of Jet Structure (1st Report, On the Difference of Jet Structure by Acoustic Excitation Modes), *Transactions of the Japan Society of Mechanical Engineers, Series B*, Vol. 54, No. 504 (1988), pp. 1938-1945 (in Japanese).
(17) Makita, H., Ohtani, H. and Ishizumi, K., Acoustic Control of Jet Structure (2nd Report, On the Streamwise Variations of Spectral Distribution and Velocity Field), *Transactions of the Japan Society of Mechanical Engineers, Series B*, Vol. 54, No. 504 (1988), pp. 1946-1952 (in Japanese).
(18) Hsiao, F. -B. and Huang, J. -M., Near-Field Flow Structures and Sideband Instabilities of an Initially Laminar Plane Jet, *Experiments in Fluids*, Vol. 9, No. 1-2 (1990), pp. 2-12.
(19) Huang, L. -S. and Ho, C. -M., Small-Scale Transition in a Plane Mixing Layer, *Journal of Fluid Mechanics*, Vol. 210 (1990), pp. 475-500.
(20) Makita, H., Matsumoto, T. and Asakura, T., Transition Process of a Two-Dimensional Jet (1st Report, Vorticity Distribution and Convection Velocity of the Vortex), *Transactions of the Japan Society of Mechanical Engineers, Series B*, Vol. 57, No. 539 (1991), pp. 2239-2246 (in Japanese).
(21) Makita, H., Matsumoto, T. and Hasegawa, T., Transition Process of a Two-Dimensional Jet (2nd Report, Comparison of Flow Visualization by a Multi-Smoke-Wire and Velocity Vector Maps), *Transactions of the Japan Society of Mechanical Engineers, Series B*, Vol. 58, No. 555 (1992), pp. 3237-3244 (in Japanese).
(22) Husain, H. and Hussain, F., Experiments on Subharmonic Resonance in a Shear Layer, *Journal of Fluid Mechanics*, Vol. 304 (1995), pp. 343-372.
(23) Makita, H., Hasegawa, T. and Sekishita, N., Turbulence Production and Energy Transfer Mechanism in the Transition Process of a Two-Dimensional Jet, *Transactions of the Japan Society of Mechanical Engineers, Series B*, Vol. 70, No. 698 (2004), pp. 2507-2514 (in Japanese).
(24) Oster, D. and Wygnanski, I., The Forced Mixing Layer between Parallel Streams, *Journal of Fluid Mechanics*, Vol. 123 (1982), pp. 91-130.
(25) Gaster, M., Kit, E. and Wygnanski, I., Large-Scale Structures in a Forced Turbulent Mixing Layer, *Journal of Fluid Mechanics*, Vol. 150 (1985), pp. 23-39.
(26) Weisbrot, I. and Wygnanski, I., On Coherent Structures in a Highly Excited Mixing Layer, *Journal of Fluid Mechanics*, Vol. 195 (1988), pp. 137-159.
(27) Zhou, M. and Wygnanski, I., The Response of a Mixing Layer Formed between Parallel Streams to a Concomitant Excitation at two Frequencies, *Journal of Fluid Mechanics*, Vol. 441 (2001), pp. 139-168.
(28) Naka, Y., Tsuboi, K., Kametani, Y., Fukagata, K. and Obi, S., Near-Field Development of a Turbulent Mixing Layer Periodically Forced by a Bimorph PVDF Film Actuator, *Journal of Fluid Science and Technology*, Vol. 5, No. 2 (2010), pp. 156-168.
(29) Tatsumi, T. and Gotoh, K., *Flow Stability Theory* (1976), p.103, Sangyo Tosho Ltd. (in Japanese).
(30) *Ibid*., p.116 (in Japanese).
(31) Brown, G. L. and Roshko, A., On Density Effects and Large Structure in Turbulent Mixing Layers, *Journal of Fluid Mechanics*, Vol. 64, Pt. 4 (1974), pp. 775-816.
(32) Moore, C. J., The Role of Shear-Layer Instability Waves in Jet Exhaust Noise, *Journal of Fluid Mechanics*, Vol. 80, Pt. 2 (1977), pp. 321-367.
(33) Taneda, S., *Fluid Mechanics Studying from Visual Pictures* (1988), p.131, Asakura Shoten Ltd. (in Japanese).
(34) Kurimoto, N., Suzuki, Y. and Kasagi, N., Active Control of Coaxial Jet Mixing with Arrayed Micro Actuators, *Transactions of the Japan Society of Mechanical Engineers,*

Series B, Vol. 70, No. 694 (2004), pp. 1417-1424 (in Japanese).

(35) Nagata, K., Sakai, Y., Shirosawa, M. and Kubo, T., Active Control of an Axisymmetric Jet Using Moving Delta-tabs (1st Report, Measurements of a Jet with Delta-tabs Moving in Phase), *Transactions of the Japan Society of Mechanical Engineers, Series B*, Vol. 73, No. 726 (2007), pp. 523-530 (in Japanese).

(36) Nagata, K., Sakai, Y., Hiromori, K., Kubo, T. and Oguro Y., Active Control of an Axisymmetric Turbulent Jet Using Moving Prominence (Effects of Shapes and Moving Patterns of the Prominence), *Transactions of the Japan Society of Mechanical Engineers, Series B*, Vol. 75, No. 754 (2009), pp. 1296-1303 (in Japanese).

(37) Schlichting, H., *Boundary-Layer Theory, 7th ed.* (1979), p. 746, McGraw-Hill.

(38) Pope, S. B., *Turbulent Flows* (2000), p. 137, Cambridge University Press.

(39) Ichimiya, M., Kamada, S., Okajima, A. and Osaki, T., Effect of Local Periodic Disturbance on Mixing Layer Downstream of Two-Dimensional Jet (Spatial structure and quantitative representation of laminar-turbulent transition process), *Transactions of the Japan Society of Mechanical Engineers, Series B*, Vol. 77, No. 779 (2011), pp. 1457-1471 (in Japanese).

(40) Sato, H., *Laminar-Turbulent Transition in Free Shear Flow*, in Tani, I. ed., *Progress in Fluid Mechanics -Turbulent Flow-* (1980), pp. 50, Maruzen (in Japanese).

(41) Rotta, J. C., Turbulent Boundary Layers in Incompressible Flow, Ferri, A., Kuchemann, D. and Sterne, L. H. G. ed., *Progress in Aeronautical Sciences* (1962), pp. 43, Pergamon Press.